Spanish Journal of Agricultural Research
13(1), e12-001, 15 pages (2015)
eISSN: 2171-9292
http://dx.doi.org/10.5424/sjar/2015131-6323
Instituto Nacional de Investigación y Tecnología Agraria y Alimentaria (INIA)

RESEARCH ARTICLE

OPEN ACCESS

Comparison among monitoring strategies to assess water flow dynamic and soil hydraulic properties in agricultural soils

Javier Valdes-Abellan[1], Joaquín Jiménez-Martínez[2], Lucila Candela[3] and Karim Tamoh[3]

[1] *University of Alicante, Department of Civil Engineering. Ctra.de San Vicente s/n. 03690 San Vicente del Raspeig (Alicante), Spain.*
[2] *Geosciences Rennes, UMR 6118 CNRS, Université de Rennes I. Rennes, France.*
[3] *Technical University of Catalonia-UPC, Department of Geotechnical Engineering and Geosciences. Barcelona, Spain.*

Abstract

Irrigated agriculture is usually performed in semi-arid regions despite scarcity of water resources. Therefore, optimal irrigation management by monitoring the soil is essential, and assessing soil hydraulic properties and water flow dynamics is presented as a first measure. For this purpose, the control of volumetric water content, θ, and pressure head, h, is required. This study adopted two types of monitoring strategies in the same experimental plot to control θ and h in the vadose zone: i) non-automatic and more time-consuming; ii) automatic connected to a datalogger. Water flux was modelled with Hydrus-1D using the data collected from both acquisition strategies independently (3820 daily values for the automatic; less than 1000 for the non-automatic). Goodness-of-fit results reported a better adjustment in case of automatic sensors. Both model outputs adequately predicted the general trend of θ and h, but with slight differences in computed annual drainage (711 mm and 774 mm). Soil hydraulic properties were inversely estimated from both data acquisition systems. Major differences were obtained in the saturated volumetric water content, θ_s, and the n and α van Genuchten model shape parameters. Saturated hydraulic conductivity, K_s, shown lower variability with a coefficient of variation range from 0.13 to 0.24 for the soil layers defined. Soil hydraulic properties were better assessed through automatic data acquisition as data variability was lower and accuracy was higher.

Additional key words: water management; Hydrus; inverse approach; water flux.

Abbreviations used: *EF* (Nash-Sutcliffe efficiency index); ET_0 (Reference evapotranspiration); *RMSE* (root mean square error); SWRC (soil water retention curve); TDR (time domain reflectometry); θ (volumetric water content); h (soil pressure head); K_{cb} (crop basal coefficient); K_e (evaporation coefficient); T_p (potential transpiration); E_p (potential evaporation); S_p (potential water uptake); $\alpha(h)$ (dimensionless water stress response function); R^2 (coefficient of determination); K_s (saturated hydraulic conductivity); α, n, l (shape factors of the van Genuchten model); θ_s (saturated volumetric water content); θ_r (residual volumetric water content); P (precipitation); I (irrigation)

Citation: Valdes-Abellan, J.; Jiménez-Martínez, J.; Candela, L.; Tamoh, K. (2015). Comparison between monitoring strategies to assess water flow dynamic and soil hydraulic properties in agricultural soils. Spanish Journal of Agricultural Research, Volume 13, Issue 1, e12-001, 15 pages. http://dx.doi.org/10.5424/sjar/2015131-6323.
Received: 27 May 2014. **Accepted:** 06 Feb 2015
http://dx.doi.org/10.5424/sjar/2015131-6323

Funding: Projects: CONSOLIDER-TRAGUA; CGL2010-22168-C03-02/BTE and CGL2013-48802-C3-3-R (Spanish Ministry of Science and Innovation)
Competing interests: The authors have declared that no competing interests exist.
Correspondence should be addressed to Javier Valdes-Abellan: javier.valdes@ua.es

Introduction

Water scarcity in arid and semi-arid regions is leading a strong competition among all sectors of water users; *e.g.,* urban, industrial or agriculture (Medwsd Working Group, 2008; Jiménez-Martínez *et al*., 2009). Efficient use of water resources is a fundamental objective in these regions, especially for agriculture, as it is the main consumer. According to future climate change predictions (IPCC, 2007; Rey *et al*., 2011; Soto-García *et al*., 2013), water scarcity could even impose constraints to society development (Lattemann & Höpner, 2008).

To increase water use efficiency in water-scarce areas, deficit irrigation has been promoted in the few last years (Aguilar *et al*., 2007; Ucar *et al*., 2009; Hussein *et al*., 2011). Information about water availability for plants is needed by planners and producers to design irrigation schemes that minimizes not only yield reductions under water-deficit conditions, but also groundwater pollution (Candela *et al*., 2007; Xu *et al*., 2009; Abrahao *et al*., 2011; Skhiri & Dechmi, 2011). Besides, caution is recommended due to the high evapotranspiration values prevailing in arid and semi-arid regions, which could result in soil salinity depending on water quality and irrigation/rainfall rates (Scanlon *et al*., 2002; Amezketa, 2007; Dahan *et al*., 2008). Therefore, hydraulic properties and water flow dynamics in agricultural soils need to carefully be assessed.

For these purposes, water dynamics monitoring and its modelling through the vadose zone are extremely important issues. Vadose zone monitoring can be performed by applying commonly used methods in the laboratory, along with a constantly growing number of field devices that follow the technological developments of recent years (SSSA, 2002; Kloss *et al.,* 2014). The most commonly used sensors range, among others, from classical ceramic cup tensiometers, with a vacuum gauge device based on the mechanical behaviour of a bourdon tube, to time domain reflectometry (TDR) assisted by gravimetric determinations of soil water content from oven-dried soil samples. After the initial manual management of *in situ* devices, more recently, sophisticated sensors with automatic data acquisition have appeared quite often, thus making monitoring less time-consuming.

In general terms, automatic and manual monitoring strategies have been separately applied to study soil water dynamics and soil hydraulic properties in different soil types to pursue different objectives (Jiménez-Martínez *et al*., 2009; Wollschläger *et al*., 2009; Wallis *et al*., 2011). However, much less attention has been paid to experimental comparative studies to simultaneously assessment of water dynamics and soil hydraulic properties by using both automatic and non-automatic monitoring devices in the same experiment. As measurement itself has not received much attention in the past, parameter estimation, and therefore appropriate measurements, is clearly the bottleneck to make further progress in today's soil physics (Durner, 2005).

The need for efficient management of water resources and optimal use of irrigation water needs careful monitoring of crucial hydrologic parameters based on different technical approaches (Bonet *et al*., 2010). The knowledge of such parameters may also allow the validation of agro-hydrological models or their improvement in order to identify efficient methodologies for estimation of crop water requirement (Rallo *et al.,* 2012, 2014; Cammalleri *et al.,* 2013). The current work presents a comparison of two different data acquisition strategies for water potential and water content monitoring at several depths. Hydrus-1D, a code for simulating water, heat, and solute movement in variably saturated media (Šimůnek *et al*., 2009), has been used to model soil water flow from automatic and non-automatic data independently. Soil hydraulic properties have been obtained by the inverse method (that is, fitting simulated data to the experimental data obtained from both acquisition strategies) and then they have been compared with laboratory estimates to assess model capability for their prediction. Finally, a comparison of drainage estimates has been made to evaluate their reliability for this purpose.

Material and methods

Field experiment and monitoring strategies

The present study was carried out in Alicante, SE Spain (38.386654N, 0.520001W), a semi-arid region where the average annual precipitation is 330 mm, and the reference evapotranspiration, ET_0, range is 1200-1400 mm with a mean summer temperature of 24.4ºC (standard deviation of 1.7ºC) and a mean winter temperature of 12.5ºC (standard deviation of 1.5ºC). For the field experiment, a 9 × 5 m plot was set up. The plot was located over an unconfined saline quaternary aquifer of detrital origin, which overlies impervious silty-clay materials dating back to the Cretaceous Period.

On the top surface, a mixture of turf grass species (St. Agustine grass, *Stenotaphrum secundatum*, and ray grass, *Lolium perenne*) was cropped to mimic current agricultural landscape management. For plot irrigation, brackish groundwater from the aquifer is currently desalted in a reverse osmosis plant. Subsequently, it is stored in a pond, where it is blended with raw groundwater. The rate of raw groundwater and desalted water mixture may range between 1:19 and 1:4 (brackish:desalted water) for winter and summer, respectively (Valdes-Abellan, 2013). Irrigation is finally carried out with the blended water. The plot is irrigated by micro-sprinklers, and this system provides a nearly uniform water input over the field experiment surface (Dechmi *et al*., 2010). This system is commonly used in this type of land cover.

Two different types of monitoring strategies adopted along a vertical profile in the vadose zone were applied in the experimental plot: non-automatic instruments, vertically installed from the surface and spatially distributed; and automatic devices (connected to a datalogger), horizontally installed from a lateral trench. The data obtained from each monitoring strategy were independently analysed and soil parameters were obtained to be compared. The monitoring process took place during 20 consecutive months.

The plot design included vertical boreholes drilled at different depths to install the non-automatic instrumentation, as well as a trench of 1.5 m in depth and 0.8 m in width, which was dug on one lateral side of the plot to install the horizontal automatic sensors (Fig. 1). After the *in situ* installation, the lateral trench wall was covered with a plastic film along its vertical extension, and was finally refilled with soil material to establish a condition of absence of flux along this plot side.

Manual instrumentation consisted in two Jet Fill tensiometers for suction measurements at 30, 45, 60, 90 and 120 cm (Soil Moisture®), and two polycarbonate access tubes of 44 mm i.d. and 1.9 m in length for soil moisture measurements with a TRIME FM TDR portable probe (IMKO®). The probe was calibrated in the laboratory following the manufacturer's recommendations. Specific calibration for the investigated soil was carried out by the comparison of volumetric water content (θ) measured by the sensors and by the gravimetric method according to Laurent *et al*. (2001, 2005) and to Varble & Chavez (2011). Tensiometers and polycarbonate access tubes were vertically installed from the top surface by hand auger equipment (Eijkelkamp®). Vertical installation was carefully performed to prevent the preferential flow associated with the devices.

Automatic data acquisition comprised a set of seven real-time monitoring devices controlled by a datalogger (Campbell Scientific®). Instrumentation consisted in: five 5TE sensors (Decagon Devices®) installed at depths of 20, 40, 60, 90 and 120 cm to take measurements of soil water content, temperature and electrical conductivity; two MPS sensors (Decagon Devices®) for the soil suction measurements at depths of 20 and 60 cm. Sensors were horizontally placed into soil media at a 40-50 cm horizontal distance from the lateral trench side (Fig. 1) in order to minimise boundary effects. Finally, the device installation holes were refilled with local soil material to reduce soil disturbance (Rothe *et al*., 1997; Ghezzehei, 2008). All the connecting wires were protected with a 16-mm flexible plastic tube to avoid instrumentation damage (Fig. 1).

Data acquisition

For the present research, data acquisition and recording started on 1 September, 2011 (day 1) and ended on 30 April, 2013 (day 608). Instrumentation was installed 8 (non-automatic) and 5 (automatic) weeks prior to beginning the monitored period in order to avoid any uncertainties associated with the equipment settlement process. For the non-automatic tensiometers, two repeated measurements were taken 3 times per week at each depth and the average value considered. Manual measurements of θ were calculated by averaging the TDR probe readings carried out twice a week (two measurements per depth in each access tube). Automatic measurements were obtained at time steps of 1-hour without replication.

The time series of precipitation, air temperature, relative humidity, wind speed and direction, barometric pressure and solar radiation were obtained from a meteorological station located 950 m from the experimental plot. All meteorological data, captured every 30 minutes, were provided by the Laboratory of Climatology (University of Alicante).

Soil profile characterisation

In order to determine the soil physical properties, five undisturbed soil cores were collected at different

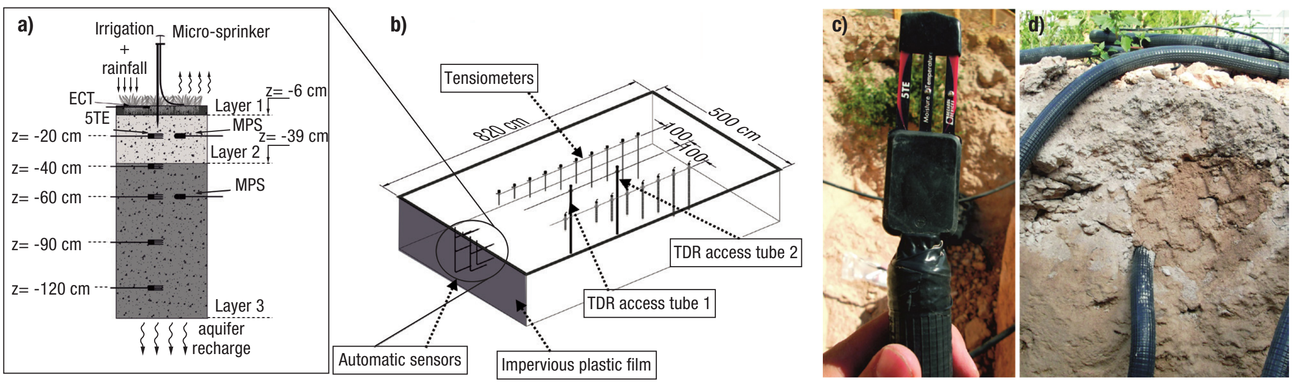

Figure 1. Scheme of the experimental plot. a) Soil profile with the automatic devices 5TE (soil water content and temperature sensor), MPS (soil water pressure head sensor) and ECT (temperature sensor); b) plot view with non-automatic devices location; c) 5TE sensor ready to be installed; and d) view of the trench and connection wires installed.

depths from three drilled boreholes. In two of them, soil samples were taken at depths of 30, 45, 60, 90 and 120 cm, whereas in the third at 20, 40, 60, 90 and 120 cm.

Soil bulk density (Grossman & Reinsch, 2002), volumetric water content (Topp & Ferré, 2002), particle size distribution (Gee & Or, 2002), saturated hydraulic conductivity (Reynolds & Elrick, 2002) and soil water retention curves (SWRC) with a ceramic plate extractor (Dane & Hopmans, 2002) were obtained at the laboratory. The unsaturated soil hydraulic parameters were: i) model fitting from the SWRC-fit code (Seki, 2007) based on the van Genuchten-Mualem constitutive relationships (Mualem, 1976; van Genuchten, 1980); ii) from Rosetta (Schaap *et al*., 2001) based on the soil textural fractions. Finally, soil mineralogy was determined by X-Ray diffractometry (Brown & Brindley, 1980; Jones, 1991).

Numerical model

Water flow

Soil water content and pressure head (θ and h, respectively) were simulated with Hydrus (Šimůnek *et al*., 2009) using the automatic and non-automatic data independently, and following the established conceptual model. Richard's equation (Richards, 1931) is the governing equation that controls the process:

$$\frac{\partial\theta}{\partial t}=\frac{\partial}{\partial z}\left(K\left(\frac{\partial h}{\partial z}+1\right)\right)-S \qquad [1]$$

where θ is the volumetric water content [$L^3 \cdot L^{-3}$], t is time [T], z is the vertical dimension [L], K is the unsaturated hydraulic conductivity of soil [$L \cdot T^{-1}$], h is the soil pressure head [L], and S is a sink term that represents water uptake by plants [$L^3 \cdot L^{-3} \cdot T^{-1}$]. The assumption of horizontal uniformity of all parameters over the experimental plot was defined.

The soil hydraulic properties were modelled based on the van Genuchten-Mualem constitutive relationships:

$$\theta(h)=\begin{cases}\theta_r+\dfrac{\theta_s-\theta_r}{\left[1+\left|\alpha h\right|^n\right]^{1-1/n}} & h<0\\ \theta_s & h\geq 0\end{cases} \qquad [2]$$

$$K(h)=K_sS_e^{\,l}\left\{1-\left[1-S_e^{\,n/(n-1)}\right]^{1-1/n}\right\}^2 \qquad [3]$$

where S_e is effective saturation:

$$S_e=\frac{\theta(h)-\theta_r}{\theta_s-\theta_r} \qquad [4]$$

and where θ_s is the saturated water content [$L^3 \cdot L^{-3}$], θ_r is the residual water content [$L^3 \cdot L^{-3}$], K_s is saturated hydraulic conductivity [$L \cdot T^{-1}$], α is the air entry parameter [L^{-1}], n is the pore size distribution parameter [-], and l is the pore connectivity parameter [-]. Parameters α, n, and l are empirical coefficients that determine the shape of the hydraulic functions. In order to avoid the number of free parameters, we defined $l = 0.5$, as commonly assumed and based on the work of Mualem (1976).

An atmospheric boundary condition was considered at the top, whereas free drainage was assumed as a lower boundary condition of the domain at a depth of 140 cm. For the upper boundary condition, the model required information on potential evapotranspiration, water input and root water uptake. A 6-cm root depth was considered constant for the selected species (St. Agustine and ray grass). The lower boundary condition was defined by considering that the water table was far below the domain.

The initial conditions considered in the modelling process were those corresponding to the measures acquired with automatic and non-automatic devices. The modelling period started 7 weeks after cropping the grass and considered a time step of 1 day. A daily average value was considered for the automatic measurements. The calibration period extended from September 2011 to November 2012 (457 monitored days), and the validation period from December 2012 to April 2013 (151 monitored days).

All the field data collected during the monitored period were analysed following a conceptual model describing the water flux through the soil-plant-atmosphere interface and the vadose zone. A similar modelling procedure was applied to the data collected from the two instrument types.

An inverse method approach was applied to obtain the soil hydraulic properties. This method yields the best fit between the observed and simulated values. The Hydrus code minimises an objective function using the Levenberg-Marquardt non-linear minimisation method (Marquardt, 1963), and it requires the definition of the minimum and maximum values of the variables that have to be considered in the process. Extreme values were fixed from the laboratory results to avoid a wide interval definition with no physical meaning. According to the methodology presented by Yakirevich *et al*. (2010), a sequential inverse procedure was performed by starting the parameter search with the first layer, while assuming that the other parameters were known (the initial estimates). The next step was to find the parameters related to the second layer. The third step involved adjusting the parameters of layers 1 and 2, simultaneously. This sequential procedure continued by gradually increasing the number of layers and, hence, the number of parameters that were simultaneously estimated. In the final step, the code searched simultaneously for all the parameters.

Potential evapotranspiration

Reference evapotranspiration, ET_0, was estimated by following the Penman-Monteith method (Allen *et al*., 1998) using the daily values of air temperature, relative humidity, wind speed and solar radiation. The reference evapotranspiration was later adapted to the local water supply and vegetal species conditions by following the dual crop coefficient approach. In this approach, two coefficients were obtained to discriminate between transpiration through plant and evaporation through the soil:

$$ET_c = \left(K_{cb} + K_e\right) ET_0 = T_p + E_P \quad [5]$$

where K_{cb} is the crop basal coefficient [-], K_e is the evaporation coefficient [-], T_p is potential transpiration [$L \cdot T^{-1}$], and E_p is potential evaporation [$L \cdot T^{-1}$].

The Penman-Monteith method discriminates between various crop growth stages with different K_{cb} values. For the selected crops, the mid-season growth stage value was considered for the whole modelled period. The percentage of soil covered by plants (80%) was obtained from the *in situ* images captured by a digital camera which were later analysed in the laboratory.

Root water uptake

The Feddes root water uptake model (Feddes *et al*., 1978) was used to simulate the water removed by plants. This term constitutes a sink of Richard's equation and defines the volume of water removed by plants per unit of time and volume of soil. In the Feddes model, the water volume removed from the soil is a function of the soil pressure head:

$$S(h) = \alpha(h) S_p \quad [6]$$

where S_p is the potential water uptake and $\alpha(h)$ is a dimensionless water stress response function ($0 \leq \alpha \leq 1$); α is assumed to be zero when it comes close to saturation due to the higher pressure head values than anaerobiosis point h_1. Zero was also assumed if the pressure head values were lower than wilting point h_3. Transpiration was optimal and the α value was 1 when actual transpiration equalled potential transpiration for the pressure head values ranging between h_2 and h_3. Transpiration increased linearly between h_1 and h_2, but also decreased linearly between h_3 and h_4.

In the simulation, a modified Feddes model (Wesseling & Brandyk, 1985) was implemented using two different h_3 values. A maximum h_3 value was considered when the transpiration rate was lower than 1 mm/day ($h_{3.1}$), and the minimum was applied when the potential transpiration rate rose above 5 mm/day ($h_{3.2}$). The appropriate h_3 value for each time step was obtained from linear interpolation at a potential transpiration rate between 1 and 5 mm/day. The values adopted for the current crop (grass) were: h_1= –10 cm; h_2= –25 cm; $h_{3.1}$= –240 cm; $h_{3.2}$= –360 cm; and h_4= –8000 cm.

Goodness-of-fit assessment

Fitting the model results to the observed data was assessed by visual inspection and statistical indicators based on the coefficient of determination (R^2) provided by the Hydrus-1D code, the root mean square error (*RMSE*) and the Nash-Sutcliffe efficiency index (*EF*). *EF* is a widely used statistical index to assess the predictive power of hydrological models (Nash & Sutcliffe, 1970).

$$RMSE = \frac{1}{x_{mean,o}} \sqrt{\frac{1}{n} \sum_{i=1}^{n} (x_{i,o} - x_{i,m})^2} \quad [7]$$

$$EF = 1 - \frac{\sum_{i=1}^{n} (x_{i,o} - x_{i,m})^2}{\sum_{i=1}^{n} (x_{i,o} - x_{mean,o})^2} \quad [8]$$

where $x_{i,o}$ is the observed value at time i, $x_{i,m}$ is the modelled value at time i, and $x_{mean,o}$ is the mean observed value.

For *RMSE,* the optimal value is zero, which is indicative of a perfect fit between the estimated and observed values, while threshold values of 0.2-0.3 are considered acceptable (Wallis *et al*., 2011). In the Nash-Sutcliffe Efficiency Index, *EF* = 1 represents a perfect fit; on the other hand *EF* = 0 results when the predicted values are as accurate as the mean of the observations and *EF*< 0 indicates that model predictions are worse than the mean of the observations. A threshold value of 0.68 was considered, which is in agreement with similar studies (Wallis *et al*., 2011).

Results

Soil characterisation

From the analysis of the soil samples from the drilled boreholes, the soil parameters estimation in the laboratory and the lateral trench inspection, three soil layers (Fig. 1) were defined in the plot. Due to the thickness of layer 1 (6 cm), the retention curve determination in the laboratory was not possible, and the soil parameters had to be obtained from textural fractions through Rosetta. For layers 2 and 3 (Fig. 1), the soil parameters were determined from laboratory retention curves and the SWRC-fit code.

According to X-Ray mineralogy, the three layers presented high calcite and quartz contents (more than 85%). Clay mineral content was practically negligible, except in the first layer where illite accounted for up to 9.7% (Table 1).

Table 2 summarises the van Genuchten-Mualem parameters K_s, α, n, θ_s and θ_r, estimated by the different procedures and for the three defined layers: a) laboratory determinations, and using Rosetta and the SWRC-FIT code; b) by inverse modelling and data from non-automatic devices; c) by inverse modelling and data from automatic devices.

Water content and pressure head measurements

The atmospheric boundary conditions, potential transpiration (T_p), potential evaporation (E_p), daily precipitation (P) and irrigation (I), recorded and computed throughout the monitored period are shown in Fig. 2. Precipitation occurred mainly in spring and autumn, and was unevenly distributed in a few intensive events, while irrigation dose was applied following climatic conditions and plant demand. T_p presented a more accentuated annual cycle according to soil water availability than E_p, which showed a smoother daily value throughout the monitored period.

Fig. 3 illustrates volumetric water content θ measured at all the monitored depths with both the automatic and non-automatic devices. Due to technical problems, some gaps exist in the time series record. The measured pressure head h displayed a similar behaviour for both the automatic and non-automatic devices (Fig. 4).

Field data quality was assessed by visual inspection and the values not considered representative were not taken into account for modelling purposes. The significant difference between the number of measurements collected from each device type is noteworthy. Automatic data acquisition provided 3,820 daily values, whereas less than 1,000 were collected in the more time-consuming non-automatic, or classical, monitoring devices for the same period.

Numerical modelling with Hydrus and water flow dynamics

Fig. 5 shows the observed and simulated θ data for the automatic and non-automatic systems. A good agreement is observed between the experimental and modelled data; simulation captured the general trend, except for the detected extreme values, as expected. Fig. 6 shows the h modelled results and field measurements for both data acquisition types. The general trends, and even some extreme events, were well pre-

Table 1. Summary of soil physical properties and mineralogy.

	Layer 1	Layer 2	Layer 3
Physical properties			
Depth (cm)	0-6	6-39	39-bottom
Textural class (USDA classification)	Clay Loam	Sandy Loam	Loam/Sandy Loam
Sand/Silt/Clay (%)	36.2/29.6/34.2	59.1/34.8/6.1	45.4/47.1/7.5
Bulk density (g/cm^3)		1.50	1.42
Porosity (–)		0.42	0.44
X-Ray mineralogy (%)			
Calcite	67.2	81.4	83.1
Quartz	18.1	9.1	7.3
Gypsum	ND	6.9	2.7
Illite	9.7	2.1	4.9
Dolomite	5	0.6	0
Albite	ND	ND	0.8
Orthoclase	ND	ND	1.0

ND: not detected

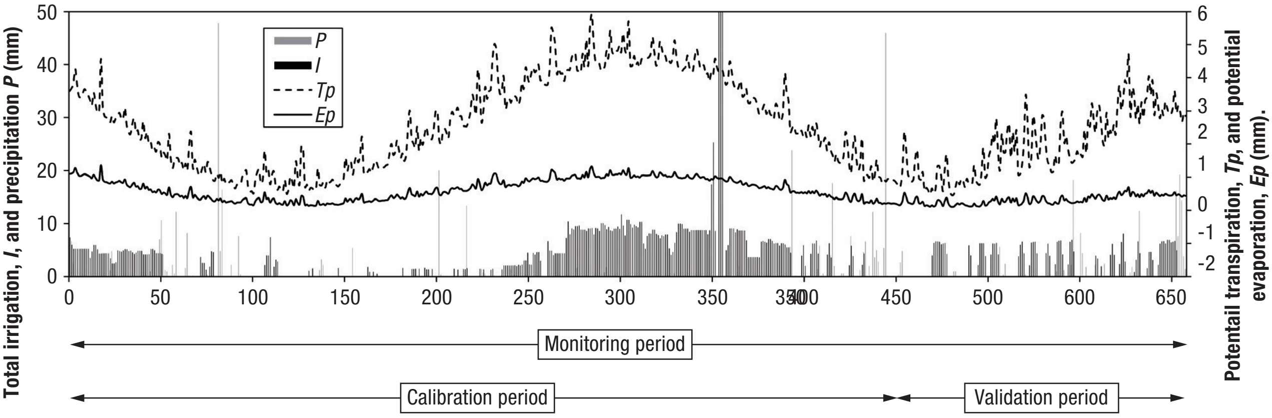

Figure 2. Potential evaporation (E_p), potential transpiration (T_p) and water input (daily precipitation, *P* and irrigation, *I*) determined during the monitored period.

Table 2. Soil hydraulic properties data obtained from the laboratory determinations and the inverse modelling with automatic and non-automatic data, using three methods.

	Layer 1			Layer 2			Layer 3		
	a	**b**	**c**	**a**	**b**	**c**	**a**	**b**	**c**
K_s (cm/day)	5.2*	4.2	5.9	51.3	66.6	62.2	35.1	50.0	60.9
θ_s (-)	0.43*	0.36	0.48	0.42	0.34	0.41	0.39	0.39	0.41
θ_r (-)	0.08*	0.04	0.04	0.18	0.17	0.20	0.17	0.15	0.15
α (cm^{-1})	$1.58\cdot10^{-2}$ *	$2.49\cdot10^{-2}$	$5.11\cdot10^{-3}$	$5.91\cdot10^{-3}$	$4.45\cdot10^{-2}$	$1.43\cdot10^{-2}$	$1.18\cdot10^{-2}$	$2.47\cdot10^{-2}$	$1.66\cdot10^{-2}$
n (-)	1.36*	1.90	1.90	1.75	1.47	1.74	1.64	1.48	1.42

Method a: laboratory determinations and the SWRC-FIT code. Method b: by inverse modelling and data from non-automatic devices. Method c: by inverse modelling and data from automatic devices. K_s, saturated hydraulic conductivity; θ_s, saturated volumetric water content; θ_r, residual volumetric water content; α, n, shape factor parameters. *: Rosetta software results based on soil textural fractions.

dicted by the model, which were also reflected by the statistics, as presented below.

Despite the good agreement obtained between the two modelled results, the flow through the lower boundary accounted for 711 mm and 774 mm from the automatic and non-automatic data, respectively, for the period from 1 September, 2011 (day 1) to 31 August, 2012 (day 366). Considering that this flow constitutes the bottom drainage to the aquifer (*i.e.,* deep percolation), the observed difference of 8.1% could be important when attempting to assess water recharge in arid or semi-arid areas.

Regarding water availability for plants, similar trend conclusions were drawn applying the model by using different experimental data sets (Fig. 7). Nevertheless, modelling by using automatic devices data resulted in a slight overestimation of water availability if compared to the other case. This highlights the fact that high frequency measurements in the field are not necessary to obtain reliable outputs for irrigation planning definition.

Fig. 8 shows the SWRCs at the depths of 20 cm (layer 2) and 60 cm (layer 3) obtained from the laboratory experiments (drying curve), as well as the corresponding estimated on the basis of inverse modelling, using data from manual and automatic devices.

Goodness-of-fit measures

Table 3 shows *RMSE*, *EF* and R^2 evaluated for *h* and θ at the monitored depths for both the devices (calibration period), as well as *RMSE* and R^2 obtained for the validation period. The values of *RMSE* and *EF* for θ do not clearly allow the identification of the best data acquisition system at the different depths or when all the data are considered. The non-automatic *EF* results gave negative values for two sensors at 90 cm and 120 cm depths (Table 3), indicating that the mean experimental value was a better predictor than simulation. This might be due to the low variability of the measurements for both data acquisition systems at these depths. If considering *h* at both depths, the *RMSE* and *EF* values indicated better adjustment for the manual acquisition data.

R^2 for the combined water content and pressure head data estimated by Hydrus gave similar results for both

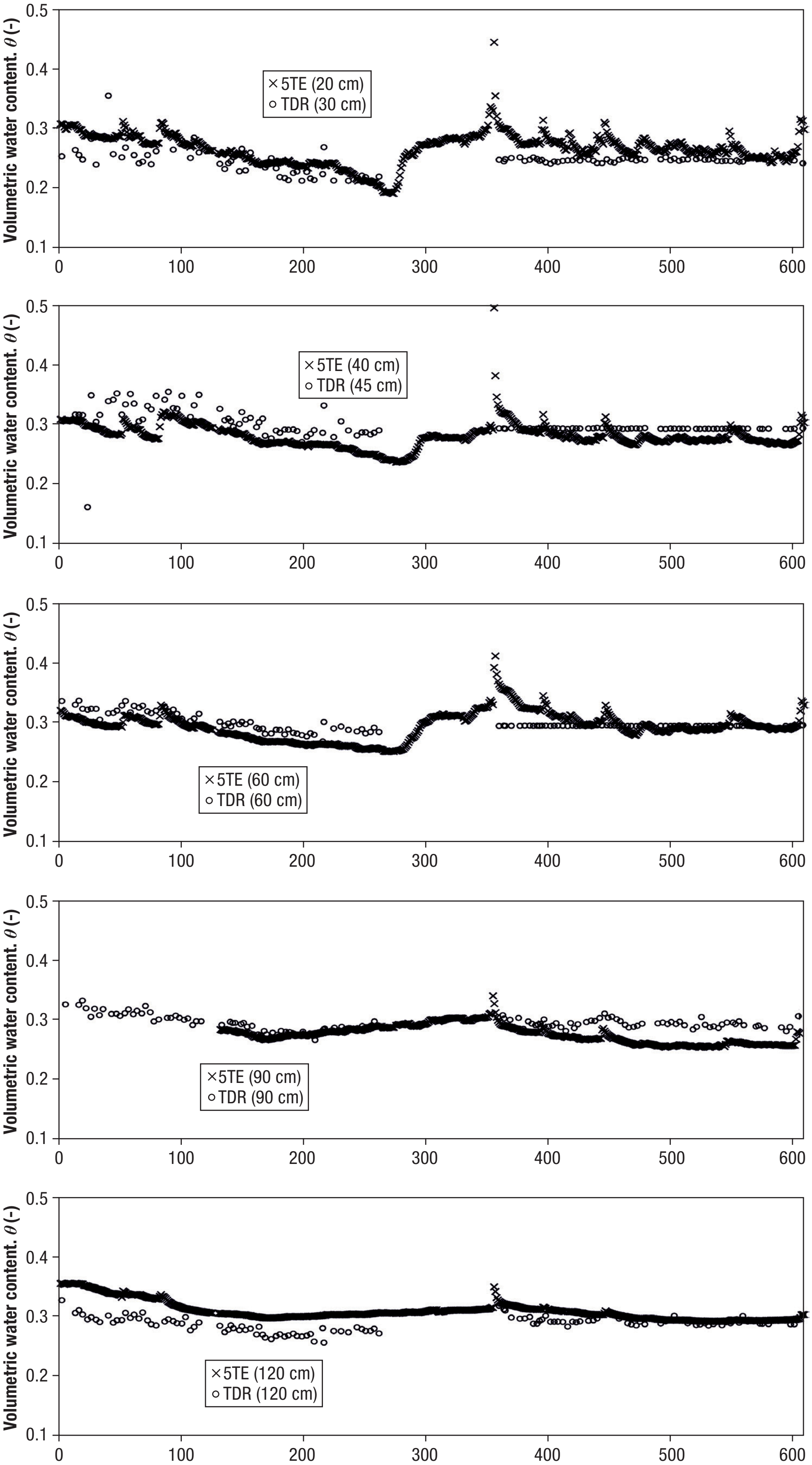

Figure 3. Volumetric water content (θ) measured with automatic and manual devices at different depths for the monitoring period.

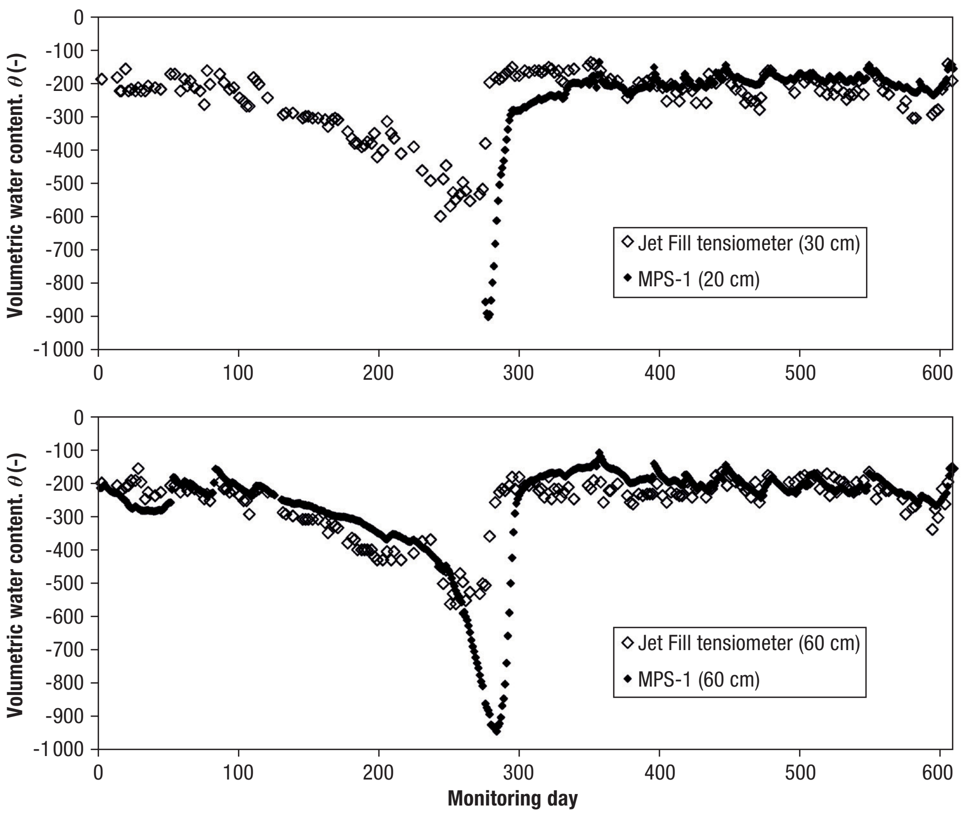

Figure 4. Soil water pressure head (*h*) measured with automatic and manual devices at the 20 cm and 60 cm depths.

the non-automatic (calibration: 0.81; validation: 0.94) and automatic (calibration: 0.98; validation: 0.98) devices, respectively; the different numbers of experimental data used in each model, which were considerably lower for the non-automatic devices could explain the observed differences.

Discussion

Data collection

Data analysis shows that water content tends to take an almost constant value, or a field capacity threshold, immediately after water input, which indicates the high hydraulic diffusivity of soil. Similar trends between the volumetric water content measurements from both types of devices were observed, except for the manual measurements at depths of 45 cm and 60 cm, which presented a flat behaviour from day 350. For the non-automatic equipment, the θ data were averaged from the two TDRs observations (TDR1 and TDR2) as horizontal homogeneity was assumed over the experimental plot. Minor differences in the volumetric water content measurements between the non-automatic (TDR1 and TDR2) and automatic sensors measurements at similar depths were observed. The differences did not follow a clear pattern among all the studied depths. They can be related to soil heterogeneity, the installation process and sensor limitations in the measured domain. Regarding the installation processes, lack of contact between soil and the polycarbonate access tube (non-automatic, TDR1 and TDR2) may lead to the presence of soil voids along the tube (West & Truss, 2006). As regards the sensors, the different soil volume controlled by the devices (3,100 and 147 cm^3 in non-automatic and automatic devices, respectively), which may contain large-sized particles, may also constitute a source of measurement uncertainty. In addition, changes in temperature and electric conductivity may have produced some alternation in the 5TE sensor readings as observed by Rosenbaum *et al.* (2010, 2011) for sensors installed at shallow soil depths.

As a general behaviour, changes in the water input on the upper boundary were first detected by the manual devices after starting irrigation following a drier winter period. The lag between the automatic and non-automatic readings can be attributed to the vertical layout of the non-automatic tensiometers since presence of a preferential flow along tensiometer length should

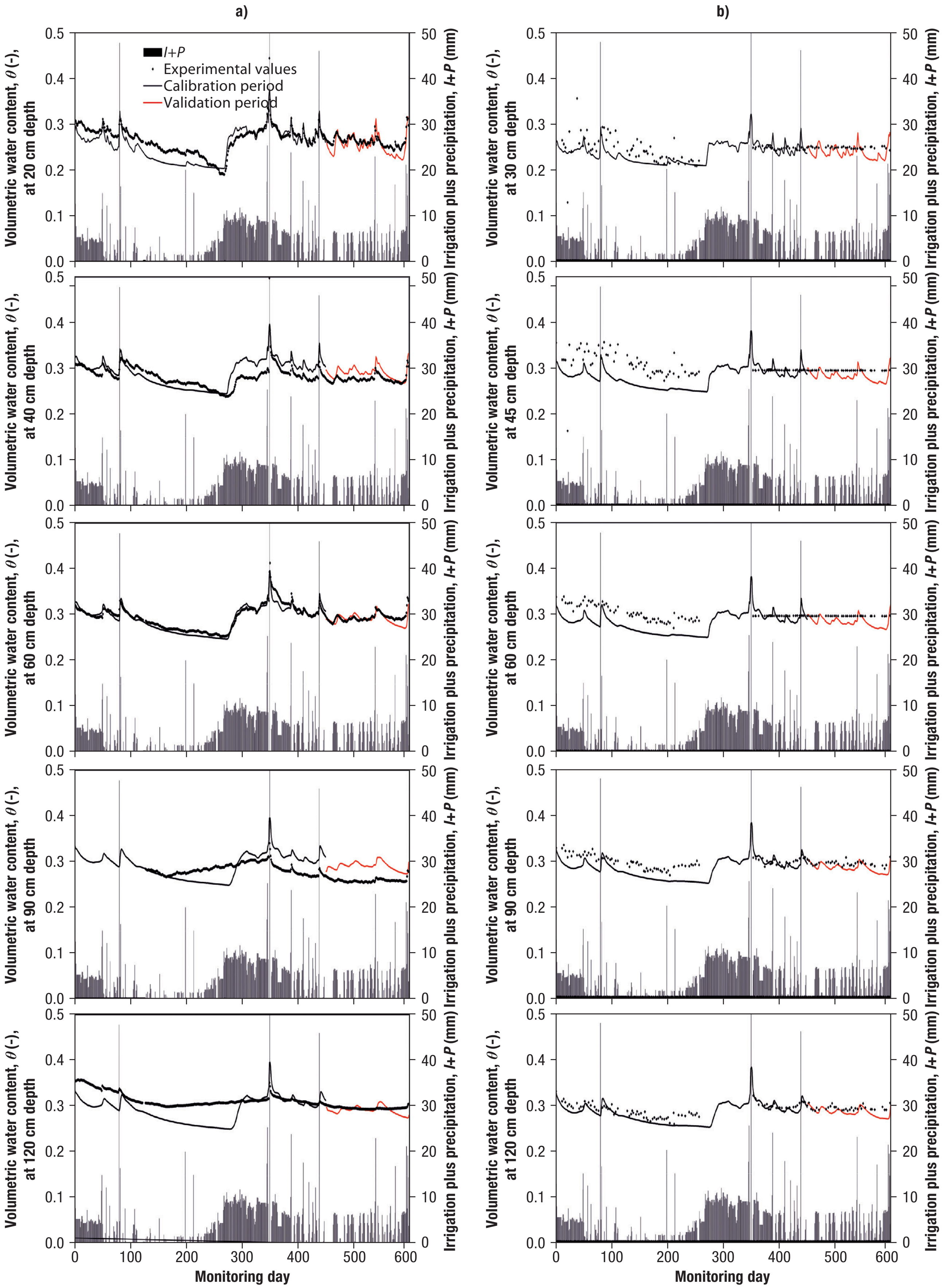

Figure 5. Observed and simulated volumetric water contents (θ) at different depths. a) Automatic data acquisition, b) manual data acquisition.

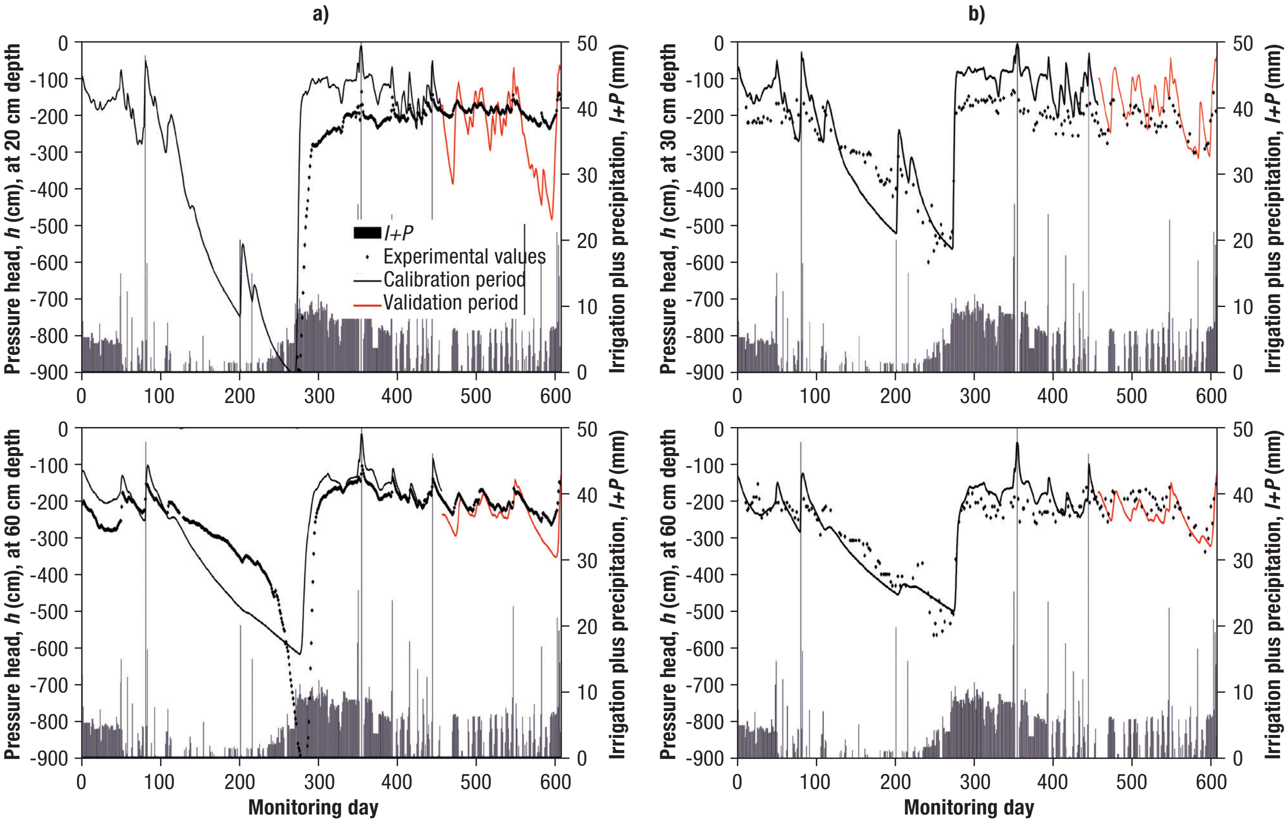

Figure 6. Observed and simulated soil water pressure heads (h) at different depths. a) Automatic data acquisition, b) manual data acquisition.

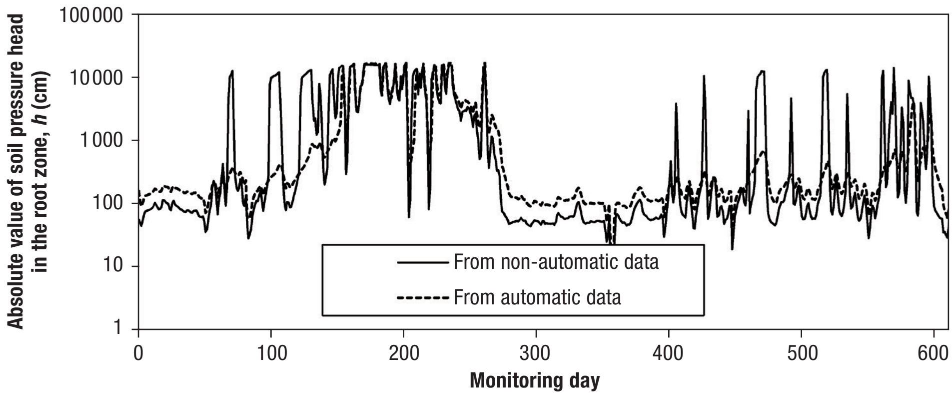

Figure 7. Absolute soil suction pressure in the root zone simulated by using the data collected by automatic and non-automatic devices.

not be ruled out. Moreover, automatic tensiometers' (MPS-1) accuracy exhibited a non-linear and uncertainty increased with h. The associated measurement of uncertainty within the −100 to −600 cm range was lower than −100 cm, and could even be higher beyond this range (Malazian *et al.*, 2011).

Soil hydraulic parameterisation

The main differences among the three soil parameterisation methods lie in the obtained θ_s, α and n values. Although differences of K_s have been generally observed in other research studies, in this research significant differences among the three methods were not observed according to the coefficient of variation values of 0.13, 0.13 and 0.24 for layers 1, 2, 3 respectively and K_s values reported in Table 2.

Based on the obtained results, it can be stated that the range of parameter values covered in the field experiments was not wide enough to obtain reliable soil water retention curves and, consequently, reliable soil parameters. However, Wollschläger *et al.* (2009) concluded that θ and h evaluated with *in situ* time series,

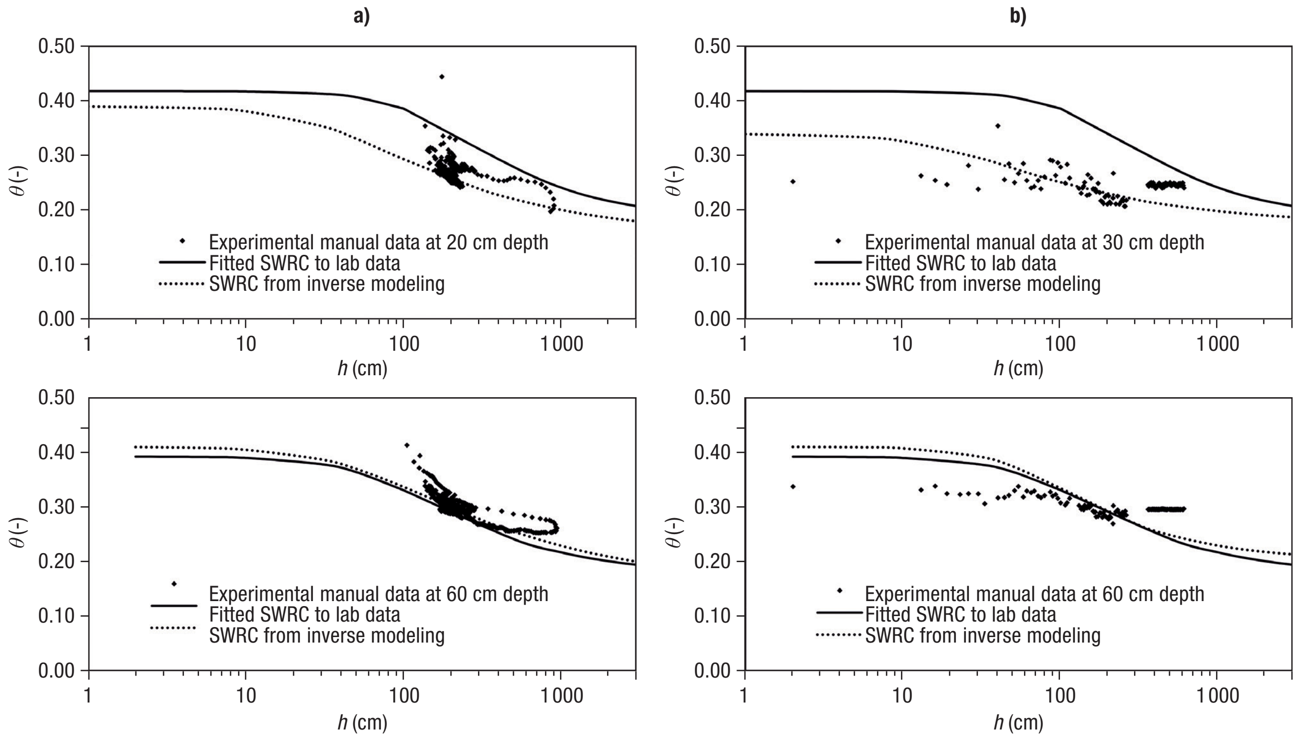

Figure 8. Soil pressure head, *h,* versus volumetric water content, *θ,* values at 20 cm and 60 cm depths acquired with the automatic (a) and manual (b) devices, along with the soil water retention curves, SWRCs, obtained from the laboratory determinations and the Hydrus inverse fitting.

Table 3. Goodness-of-fit results.

Acquisition	Statistics	Pressure head, *h*			Volumetric water content, *θ*						All (*h* and *θ*)
		20 cm	60 cm	All	30 cm	45 cm	60 cm	90 cm	120 cm	All	
Automatic	*RMSE*	0.65	0.41	0.48	0.08	0.07	0.03	0.10	0.10	0.08	
	EF	–0.39	0.49	0.3	0.54	0.12	0.89	–4.54	–3.31	0.32	
	R^2										0.81
	RMSE validation	0.52	0.21	0.38	0.05	0.05	0.03	0.13	0.04	0.06	
	R^2 validation										0.94
Non-automatic	*RMSE*	0.3	0.16	0.24	0.11	0.13	0.10	0.08	0.05	0.10	
	EF	0.48	0.8	0.63	0.00	0.43	0.24	–0.02	–0.37	0.12	
	R^2										0.98
	RMSE validation	0.29	0.18	0.24	0.07	0.06	0.05	0.04	0.04	0.05	
	R^2 validation										0.98

RMSE: root mean square error. *EF*: Nash-Sutcliffe efficiency index. R^2: coefficient of determination.

along with inverse modelling, were suitable for determining soil hydraulic characteristics. Moreover, the SWRCs estimated from the field data, unlike those data obtained from the laboratory, were generally determined under transient conditions, which confers uncertainty to the final results, as well as differences of soil volume between the soil cores analysed in the laboratory and the volume considered by the sensors.

Regarding K_s, and by presenting a range of several orders of magnitude, similar values were obtained for all the layers and parameterisation approaches. The parameters obtained with Rosetta for layer 1 showed that pedotransfer functions can be a useful tool when laboratory determinations are not provided. However, in order to reduce uncertainty with soil hydraulic parameters, pedotransfer functions should be combined with other currently applied parameter determination techniques.

Soil parameterisations through inverse flow modelling from both data types gave similar results despite the data length record and variability. Accordingly, both the applied data acquisition methodologies proved useful and were equally accurate for assessing *in situ* water flux dynamics.

Field monitoring for irrigation dose demand is crucial for avoiding plant stress and water resources sustainability in order to prevent water losses by deep infiltration or further groundwater pollution consequences. The need for efficient irrigation management implies agricultural system knowledge, and also the appropriate technologies and methods to be applied for accurate soil media measurements. The results obtained from this study provide some insights into soil and vadose zone monitoring strategies to assess water dynamics and soil hydraulic properties.

Field research and hydraulic parameters monitoring offer the complexity of profiling values in soil depths. One of the main limitations of the present work is certainly our inability to measure effective properties to describe the overall system; used devices for hydraulic parameters monitoring only provide information for a small soil volume to describe the average properties of the complete profile.

The observations made with the vertical-installed instruments need to be carefully analysed as the installation process can lead to preferential flow paths, and to lack of contact between the device wall and soil media, which can distort the observed values, which would not likely to be detected by our sensors if only one monitoring strategy type was considered. It is not clear whether conclusive measurements can be taken despite reasonable efforts made, especially when it is necessary to quantify extreme heterogeneity phenomena, such as preferential flow.

The laboratory determinations of soil hydraulic properties better fit the experimental measurements (from both the automatic and non-automatic sensors) than the soil hydraulic properties inferred from inverse modelling fit the laboratory results. It should be noticed that if previous information on soil characteristics from laboratory determinations are not considered, unrealistic soil hydraulic parameters from modelling approaches may be obtained.

Hydrus simulations were able to mimic the responses of a field-scale instrumented plot with the automatic and manual data acquisition systems. The statistical results and visual inspection showed a good agreement between the predicted and the observed values in θ and h, even with a major difference in the number of observations associated to the different strategies of data collection.

Nevertheless, the θ and h trends were better predicted than extreme episodes, a fact that has also been observed by other researchers. The goodness-of-fit values showed slight differences between the modelled parameters from the manual and automatic experimental data. The fit of the θ data was slightly better than for the h data. This fact may be related to the equilibrium time with soil required by the pressure head devices to obtain accurate measurements.

From the obtained results, it is stated that selection between automatic and manual devices has to be based on the particular research objective. Time-consuming data acquisition (longer with manual equipment) and high equipment acquisition costs (for the automatic devices) both appear to be the most important aspects when finally selecting instrumentation. From an irrigation management viewpoint, no significant differences are highlighted between the two investigated strategies. However, soil hydraulic properties may be better assessed through automatic acquisition as data variability and accuracy are lower than by the non-automatic type. Moreover, the differences in the bottom drainage value obtained by considering the two different data acquisition systems highlight the variability of this assessment to similar experimental data.

Acknowledgements

The authors are grateful to Dr. G. González-Barberá and Mr. A. Zamora from the Department of Soil and Water Conservation (CEBAS-CSIC, Murcia, Spain), to Mr. I. Queralt from the Institute of Earth Sciences Jaume Almera Institute (ICTJA-CSIC, Barcelona, Spain), and to Mr. J.L. Romeu and Mr. F. Gómez Sánchez for their collaboration in this study. Gratitude is also expressed to the University of Alicante.

References

Abrahao R, Sarasa J, Causape J, Garcia-Garizabal I, Ovelleiro JL, 2011. Influence of irrigation on the occurrence of organic and inorganic pollutants in soil, water and sediments of a Spanish agrarian basin (Lerma). Span J Agric Res 9 (1): 124-134. http://dx.doi.org/10.5424/sjar/20110901-208-10.

Aguilar M, Borjas F, Espinosa M, 2007. Agronomic response of maize to limited levels of water under furrow irrigation in southern Spain. Span J Agric Res 5 (4): 587-592. http://dx.doi.org/10.5424/sjar/2007054-280.

Allen RG, Pereira LS, Raes D, Martin S, 1998. Crop evapotranspiration: guidelines for computing crop water requirements. FAO Irrig Drain Papers nº56. FAO, Rome. 326 pp.

Amezketa E, 2007. Soil salinity assessment using directed soil sampling from a geophysical survey with electromagnetic technology: A case study. Span J Agric Res 5 (1): 91-101. http://dx.doi.org/10.5424/sjar/2007051-225.

Bonet L, Ferrer P, Castel JR, Intrigliolo DS, 2010. Soil capacitance sensors and stem dendrometers. useful tools for irrigation scheduling of commercial orchards? Span J Agric Res 8 (Suppl. 2): S52-S65. http://dx.doi.org/10.5424/sjar/201008S2-1348.

Brown G, Brindley GW, 1980. X-ray diffraction procedures for clay mineral identification. In: Crystal structure of clay minerals and their x-ray identification. Mineral Soc Mon 5 (Brindley GW, Brown G, eds.). Mineralogical Society, London, pp: 305-360.

Cammalleri C, Agnese C, Ciraolo G, Minacapilli M, Provenzano G, 2013. Combined use of eddy covariance and sap flow techniques for partition of ET fluxes and water stress assessment in an irrigated olive orchard. Agr Water Manage 120: 89-97. http://dx.doi.org/10.1016/j.agwat.2012.10.003.

Candela L, Fabregat S, Josa A, Suriol J, Vigués N, Mas J, 2007. Assessment of soil and groundwater impacts by treated urban wastewater reuse. A case study: Application in a golf course (Girona, Spain). Sci Total Environ 374 (1): 26-35. http://dx.doi.org/10.1016/j.scitotenv.2006.12.028.

Dahan O, Tatarsky B, Enzel Y, Kulls C, Seely M, Benito G, 2008. Dynamics of flood water infiltration and ground water recharge in hyperarid desert. Ground water 46 (3): 450-461. http://dx.doi.org/10.1111/j.1745-6584.2007.00414.x.

Dane JH, Hopmans JW, 2002. Pressure plate extractor. In: Methods of soil analysis, Part 4. Physical methods (Dane J, Topp C, eds). Soil Sci Soc Am, Madison (WI, USA), pp: 688-690.

Dechmi F, Playan E, Faci J, Cavero J, 2010. Simulation of sprinkler irrigation water uniformity impact on corn yield. Span J Agric Res 8 (Suppl. 2): S143-S151. http://dx.doi.org/10.5424/sjar/201008S2-1357.

Durner W, 2005. Study unit S2-5. Solute Transport in the Unsaturated Zone. Technische Universität Braunschweig, Institut für Geoökologie, 61 pp. Available in: http://www.soil.tu-bs.de/lehre/Skripte/2005.Durner.PROWATER.S2-5.Transport%20and%20Accessibility.pdf [28 January 2015].

Feddes RA, Kowalik PJ, Zaradny H, 1978. Simulation of field water use and crop yield. Wiley, NY, USA. 188 pp.

Gee GW, Or D, 2002. Particle-size analysis. In: Methods of soil analysis, Part 4. Physical methods (Dane J, Topp C, eds). Soil Sci Soc Am, Madison (WI, USA), pp: 255-293.

Ghezzehei TA, 2008. Errors in determination of soil water content using time domain reflectometry caused by soil compaction around waveguides. Water Resour Res 44 (8): W08451. http://dx.doi.org/10.1029/2007WR006502.

Grossman RB, Reinsch TG, 2002. Bulk density and linear extensibility. In: Methods of soil analysis, Part 4. Physical methods (Dane J, Topp C, eds). Soil Sci Soc Am, Madison (WI, USA), pp: 201-228.

Hussein F, Janat M, Yakoub A, 2011. Simulating cotton yield response to deficit irrigation with the FAO AquaCrop model. Span J Agric Res 9 (4): 1319-1330. http://dx.doi.org/10.5424/sjar/20110904-358-10.

IPCC, 2007. Climate Change 2007: Synthesis report. Intergovernmental Panel On Climate Change, Geneva (Switzerland). Available in http://www.ipcc.ch/publications_and_data/ar4/syr/en/contents.html [28 January 2015].

Jiménez-Martínez J, Skaggs TH, van Genuchten MT, Candela L, 2009. A root zone modelling approach to estimating groundwater recharge from irrigated areas. J Hydrol 367 (1-2): 138-149. http://dx.doi.org/10.1016/j.jhydrol.2009.01.002.

Jones A, 1991. X-Ray fluorescence analysis. In: Soil analysis. Modern instrumental techniques (Smith KA, ed.). Marcel Dekker, NY, USA, pp: 287-324.

Kloss S, Schùltze N, Schmidhalter U, 2014. Evaluation of very high soil water tension threshold values in sensor based deficit irrigation systems. J Irrig Drain Eng 140(9), A4014003. http://dx.doi.org/10.1061/(ASCE)IR.1943-4774.0000722.

Lattemann S, Höpner T, 2008. Environmental impact and impact assessment of seawater desalination. Desalination 220 (1-3): 1-15. http://dx.doi.org/10.1016/j.desal.2007.03.009.

Laurent JP, Ruelle P, Bréda N, Chanzy A, Chevallier C, 2001. On the use of the TDR TRIME-TUBE system for profiling water content in soils. TDR'01 Proc 2nd Int Symp Workshop on time domain reflectometry for innovative geotechnical applications (Dowding CH, McGarry SM, Evanstons SE, eds.). Illinois (USA), pp: 1-10.

Laurent JP, Ruelle P, Delage L, Zaïri A, Nouna BB, Adjmi T, 2005. Monitoring soil water content profiles with a commercial TDR system. Vadose Zone J 4(4): 1030-1036. http://dx.doi.org/10.2136/vzj2004.0144.

Malazian A, Hartsough P, Kamai T, Campbell GS, Cobos DR, Hopmans JW, 2011. Evaluation of MPS-1 soil water potential sensor. J Hydrol 402(1-2): 126-134. http://dx.doi.org/10.1016/j.jhydrol.2011.03.006.

Marquardt D, 1963. An algorithm for least-squares estimation of nonlinear parameters. SIAM J Appl Math 11 (2): 431-441. http://dx.doi.org/10.1137/0111030.

Medwsd Working Group, 2008. Mediterranean Water Scarcity and Drought Report. European Commission. Euro-Mediterranean Information System on know-how in the Water sector. Available in http://www.semide.net/topics/WaterScarcity/EUWI_WSD_Report_FINAL_June_2008.pdf [28 January 2015].

Mualem Y, 1976. A new model for predicting the hydraulic conductivity of unsaturated porous media. Water Resour Res 12(3): 513-522. http://dx.doi.org/10.1029/WR012i003p00513.

Nash JE, Sutcliffe JV, 1970. River flow forecasting through conceptual models, Part I. A discussion of principles. J Hydrol 10(3): 282-290. http://dx.doi.org/10.1016/0022-1694(70)90255-6.

Rallo G, Agnese C, Minacapilli M, Provenzano G, 2012. Comparison of SWAP and FAO agro-hydrological models to schedule irrigation of wine grape. J Irrig Drain Eng 138(1): 581-591. http://dx.doi.org/10.1061/(ASCE)IR.1943-4774.0000435.

Rallo G, Baiamonte G, Manzano Juárez J, Provenzano G, 2014. Improvement of FAO-56 model to estimate transpiration fluxes of drought tolerant crops under soil water deficit: application for olive groves. J Irrig Drain Eng 140(9): 1-8. http://dx.doi.org/10.1061/(ASCE)IR.1943-4774.0000693.

Rey D, Garrido A, Mínguez MI, Ruiz-Ramos M, 2011. Impact of climate change on maize's water needs, yields and profitability under various water prices in Spain. Span J Agric Res 9(4): 1047-1058. http://dx.doi.org/10.5424/sjar/20110904-026-11.

Reynolds WD, Elrick DE, 2002. Constant head soil core (tank) method. In: Methods of soil analysis, Part 4.

Physical methods (Dane J, Topp C, eds). Soil Sci Soc Am, Madison (WI, USA), pp: 804-808.

Richards LA, 1931. Capillary conduction of liquids through porous mediums. J Appl Phys 1(5): 318-333.

Rosenbaum U, Huisman JA, Weuthen A, Vereecken H, Bogena HR, 2010. Sensor-to-sensor variability of the ECH2o EC-5, TE, and 5TE sensors in dielectric liquids. Vadose Zone J 9(1): 181-186. http://dx.doi.org/10.2136/vzj2009.0036.

Rosenbaum U, Huisman JA, Vrba J, Vereecken H, Bogena HR, 2011. Correction of temperature and electrical conductivity effects on dielectric permittivity measurements with ECH 2O sensors. Vadose Zone J 10(2): 582-593. http://dx.doi.org/10.2136/vzj2010.0083.

Rothe A, Weis W, Kreutzer K, Matthies D, Hess U, Ansorge B, 1997. Changes in soil structure caused by the installation of time domain reflectometry probes and their influence on the measurement of soil moisture. Water Resour Res 33(7): 1585-1593. http://dx.doi.org/10.1029/97WR00677.

Scanlon BR, Healy RW, Cook PG, 2002. Choosing appropriate techniques for quantifying groundwater recharge. Hydrogeol J 10(1): 18-39. http://dx.doi.org/10.1007/s10040-001-0176-2.

Schaap MG, Leij FJ, van Genuchten MT, 2001. Rosetta: A computer program for estimating soil hydraulic parameters with hierarchical pedotransfer functions. J Hydrol 251(3-4): 163-176. http://dx.doi.org/10.1016/S0022-1694(01)00466-8.

Seki K, 2007. SWRC fit - A nonlinear fitting program with a water retention curve for soils having unimodal and bimodal pore structure. Hydrol Earth Syst Sci Discuss 4(1): 407-437. http://dx.doi.org/10.5194/hessd-4-407-2007.

Šimůnek J, Šejna M, Saito H, Sakai M, van Genuchten MT, 2009. The Hydrus-1D software package for simulating the movement of water, heat, and multiple solutes in variability saturated media, v. 4.08. Dept Environ Sci, Univ California, Riverside, CA, USA. Available in http://www.pc-progress.com/Downloads/Pgm_hydrus1D/HYDRUS1D-4.08.pdf [28 January 2015].

Skhiri A, Dechmi F, 2011. Irrigation return flows and phosphorus transport in the middle Ebro River Valley (Spain). Span J Agric Res 9 (3): 938-949. http://dx.doi.org/10.5424/sjar/20110903-360-10.

Soto-García M, Martínez-Alvarez V, García-Bastida PA, Alcon F, Martin-Gorriz B, 2013. Effect of water scarcity and modernisation on the performance of irrigation districts in south-eastern Spain. Agr Water Manage 124: 11-19. http://dx.doi.org/10.1016/j.agwat.2013.03.019.

SSSA, 2002. Methods of soil analysis. Part 4. Physical methods. SSSA Series. Soil Sci Soc Am, Madison, USA, 1692 pp.

Topp GC, Ferré PA, 2002. Thermogravimetric using convective oven-drying. In: Methods of soil analysis, Part 4. Physical methods (Dane J, Topp C, eds). Soil Sci Soc Am, Madison (WI, USA), pp: 422-424.

Ucar Y, Kadayifci A, Yilmaz HI, Tuylu GI, Yardimci N, 2009. The effect of deficit irrigation on the grain yield of dry bean (Phaseolus vulgaris L.) in semiarid regions. Span J Agric Res 7 (2): 474-485. http://dx.doi.org/10.5424/sjar/2009072-1498.

Valdes-Abellan J, 2013. Estudio de los impactos sobre la zona no saturada derivados del uso de agua desalada procedente de acuíferos salobres continentales. Study of impacts on the vadose zone deriving from use of brackish inland aquifers desalted water. Doctoral Thesis. Univ Alicante, Spain. [In English].

van Genuchten MT, 1980. Closed-form equation for predicting the hydraulic conductivity of unsaturated soils. Soil Sci Soc Am J 44(5): 892-898. http://dx.doi.org/10.2136/sssaj1980.03615995004400050002x.

Varble JL, Chávez JL, 2011. Performance evaluation and calibration of soil water content and potential sensors for agricultural soils in eastern Colorado. Agr Water Manage 101(1): 93-106. http://dx.doi.org/10.1016/j.agwat.2011.09.007.

Wallis KJ, Candela L, Mateos RM, Tamoh K, 2011. Simulation of nitrate leaching under potato crops in a Mediterranean area. Influence of frost prevention irrigation on nitrogen transport. Agr Water Manage 98(10): 1629-1640. http://dx.doi.org/10.1016/j.agwat.2011.06.001.

Wesseling JG, Brandyk T, 1985. Introduction of the occurrence of high groundwater levels and surface water storage in computer program SWATRE. ICW, Wageningen, The Netherlands, 46 pp. Available in http://library.wur.nl/WebQuery/wurpubs/425271 [28 January 2015].

West J, Truss SW, 2006. Borehole time domain reflectometry in layered sandstone: Impact of measurement technique on vadose zone process identification. J Hydrol 319(1-4): 143-162. http://dx.doi.org/10.1016/j.jhydrol.2005.06.033.

Wollschläger U, Pfaff T, Roth K, 2009. Field-scale apparent hydraulic parameterisation obtained from TDR time series and inverse modelling. Hydrol Earth Syst Sci 13(10): 1953-1966. http://dx.doi.org/10.5194/hess-13-1953-2009.

Xu J, Chen W, Wu L, Green R, Chang AC, 2009. Leachability of some emerging contaminants in reclaimed municipal wastewater-irrigated turf grass fields. Environ Toxicol Chem 28(9): 1842-1850. http://dx.doi.org/10.1897/08-471.1.

Yakirevich A, Gish TJ, Šimůnek J, van Genuchten MT, Pachepsky YA, Nicholson TJ, Cady RE, 2010. Potential impact of a seepage face on solute transport to a pumping well. Vadose Zone J 9(3): 686-696. http://dx.doi.org/10.2136/vzj2009.0054.